Chemotherapy Response Evaluation with ^{18}F-FDG PET in Patients with Non-Small Cell Lung Cancer

Lioe-Fee de Geus-Oei[1], Henricus F.M. van der Heijden[2], Eric P. Visser[1], Rick Hermsen[1], Bas A. van Hoorn[1], Johanna N.H. Timmer-Bonte[2,3], Antoon T. Willemsen[4], Jan Pruim[4], Frans H.M. Corstens[1], Paul F.M. Krabbe[5], and Wim J.G. Oyen[1]

[1]Department of Nuclear Medicine, Radboud University Nijmegen Medical Centre, Nijmegen, The Netherlands; [2]Department of Pulmonary Diseases, Radboud University Nijmegen Medical Centre, Nijmegen, The Netherlands; [3]Department of Medical Oncology, Radboud University Nijmegen Medical Centre, Nijmegen, The Netherlands; [4]Department of Nuclear Medicine and Molecular Imaging, University Medical Center Groningen, Groningen, The Netherlands; and [5]Department of Medical Technology Assessment, Radboud University Nijmegen Medical Centre, Nijmegen, The Netherlands

The aim of this prospective study was to evaluate the value of ^{18}F-FDG PET for the assessment of chemotherapy response in patients with non–small cell lung cancer. Furthermore, part of the objective of this study was to compare 2 methods to quantify changes in glucose metabolism. **Methods:** In 51 patients, dynamic ^{18}F-FDG PET was performed before and at 5–8 wk into treatment. Simplified methods to measure glucose metabolism (standardized uptake value [SUV]) and quantitative measures (metabolic rate of glucose [MR_{Glu}]), derived from Patlak analysis, were evaluated. The overall survival and progression-free survival with respect to MR_{Glu} and SUV were calculated using Kaplan–Meier estimates. Fractional changes in tumor glucose use were stratified by the median value and also the predefined EORTC (European Organization for Research and Treatment of Cancer) metabolic response criteria, and criteria applying cutoff levels similar to those of RECIST (Response Evaluation Criteria in Solid Tumors) were evaluated. **Results:** When stratifying at the median value of ΔMR_{Glu} and ΔSUV, the difference in overall survival ($P = 0.017$ for ΔMR_{Glu}, $P = 0.018$ for ΔSUV) and progression-free survival ($P = 0.002$ for ΔMR_{Glu}, $P = 0.0009$ for ΔSUV) was highly significant. When applying the predefined criteria for metabolic response, the cutoff levels as also used for size measurement (RECIST) showed significant differences for ΔSUV between response categories in progression-free survival ($P = 0.0003$) as well as overall survival ($P = 0.027$). **Conclusion:** The degree of chemotherapy-induced changes in tumor glucose metabolism as determined by ^{18}F-FDG PET is highly predictive for patient outcome, stratifying patients into groups with widely differing overall survival and progression-free survival probabilities. The use of ^{18}F-FDG PET for therapy monitoring seems clinically feasible, because simplified methods to measure tumor glucose use (SUV) are sufficiently reliable and can replace more complex, quantitative measures (MR_{Glu}) in this patient population.

Molecular imaging with ^{18}F-FDG PET has an established role in the standard of care in presurgical staging of patients with non–small cell lung cancer (NSCLC). The addition of ^{18}F-FDG PET to the diagnostic work-up has been shown to significantly reduce the number of futile mediastinoscopies and thoracotomies (*1–3*). ^{18}F-FDG PET has also demonstrated its potential in radiation treatment planning and detection of recurrent disease (*4–7*).

Nowadays, there is an increasing interest in the role of ^{18}F-FDG PET beyond staging, such as the prediction of tumor response to therapy. Response assessment with morphologic imaging techniques has limitations in reliably distinguishing necrotic tumor or fibrotic scar from residual tumor tissue (*8*). Indeed, final treatment outcome will be determined more by the biologic aggressiveness of residual tumor than by its volume (*9*). Furthermore, some new therapies may be cytostatic instead of cytoreductive, in which case successful treatment may not lead to a decrease in tumor size and thus poses new demands on imaging modalities.

^{18}F-FDG PET is ideally suited to overcome these kinds of problems. One of the advantages of ^{18}F-FDG PET is that it not only can visualize but also can quantify ^{18}F-FDG uptake to distinguish metabolically highly active from less-active tumor tissues. Furthermore, metabolic alterations of tumor cells, indicative of tumor response to therapy, may occur before alterations in tumor size. Early prediction of tumor response is of particular interest in patients with advanced stages of NSCLC. Tumor progression during first-line chemotherapy occurs in approximately 30% of patients (*10*). Because of relatively slow tumor shrinkage, as measured on morphologic

imaging modalities, a significant percentage of patients will continue to undergo toxic therapy for weeks without benefit.

In the present prospective study, a design was used that allowed for comparative analysis of different quantitative PET methods to measure tumor glucose use at various levels of complexity. Furthermore, prospective as well as post hoc definitions for metabolic response were assessed to evaluate the value of ^{18}F-FDG PET in therapy response monitoring of NSCLC.

MATERIALS AND METHODS

Patient Eligibility Criteria

Between March 2002 and December 2005, all patients in the Radboud University Nijmegen Medical Centre with any stage of NSCLC and measurable tumor lesions according to the Response Evaluation Criteria in Solid Tumors (RECIST)—who were scheduled to undergo induction chemotherapy or chemotherapy in a palliative setting—were offered the opportunity to participate in the study. Initial staging was performed according to the guidelines of the American Society of Clinical Oncology (11). Exclusion criteria were diabetes mellitus and pregnancy. In all patients, treatment decision making was done by a multidisciplinary team, including cardiothoracic surgeons, pulmonologists, medical oncologists, radiation oncologists, pathologists, radiologists, and nuclear medicine physicians. Clinicians had access to the pretreatment staging static whole-body PET scan but were unaware of the results of the dynamic ^{18}F-FDG PET scans. The study was approved by the Institutional Review Board of the Radboud University Nijmegen Medical Centre, and written informed consent was obtained from each patient.

Quantitative Dynamic ^{18}F-FDG PET Data Acquisition and Reconstruction

Dynamic ^{18}F-FDG PET was performed at baseline and after the second or third cycle of chemotherapy, depending on the chemotherapy regimen. The median interval between the clinical-staging ^{18}F-FDG PET and the baseline dynamic ^{18}F-FDG PET was 3 d. Patients fasted for at least 6 h before imaging. Intake of noncaloric beverages was permitted. All scans were acquired on an ECAT-EXACT47 PET scanner (Siemens Medical Solutions). The field of view for dynamic acquisition was based on whole-body ^{18}F-FDG PET and CT scans performed for initial staging, including as many measurable tumor lesions as possible. A 20-min transmission scan was made, using the internal ^{68}Ge/^{68}Ga sources, to correct for photon attenuation. Approximately 200 MBq ^{18}F-FDG were injected intravenously over a 1-min period, using a constant-infusion remote-controlled pump (Medrad). The dynamic data acquisition, performed in septa-extended (2-dimensional) mode, was started simultaneously with the injection of ^{18}F-FDG and consisted of 16 time frames with variable frame length (10×30 s, 3×300 s, 3×600 s) for a total time of 50 min. A more detailed description of the data acquisition, reconstruction, and analysis methods was published previously (12).

Plasma Time–Activity Curves

To measure the blood clearance of ^{18}F-FDG, plasma time–activity curves were derived from arterial blood sampling when feasible. Arterial blood samples were taken manually at set times to provide an arterial plasma input function as described previously (12). When arterial cannulation was contraindicated or not feasible, an image-based input function was determined by measuring

^{18}F-FDG counts in a volume of interest (VOI) over the ascending aorta, which accurately determines ^{18}F-FDG blood levels (12).

Tumor Time–Activity Curves

Tumor time–activity curves were obtained by placing VOIs semiautomatically over the tumor and metastases using a threshold of 50% of the maximum pixel value within the lesion. Necrotic areas were excluded from the VOIs. A volume-weighted mean value of tumor glucose use (metabolic rate of glucose [MR_{glu}]) of all lesions in each PET scan was derived to provide one value for each study. VOIs drawn on the first ^{18}F-FDG PET (before initiation of chemotherapy) were copied to the second ^{18}F-FDG PET (after 2 or 3 cycles of chemotherapy).

Patlak Graphical Analyses

For quantitative measurement of glucose metabolism, Patlak graphical analysis was used to calculate the MR_{Glu} (expressed in $\mu mol \cdot mL^{-1} \cdot min^{-1}$) in tumor tissue (13,14). A detailed description of the Patlak graphical analyses and its assumptions have been published elsewhere (12,13). In brief, the Patlak approach takes into account differences in the whole-body distribution of ^{18}F-FDG at the time of scanning, which may affect the accumulation of ^{18}F-FDG in the tumor tissue. Furthermore, the MR_{Glu} in tumor was calculated by multiplication of the slope of the Patlak plot and the basic blood glucose level (expressed in $\mu mol \cdot mL^{-1}$). Blood glucose level was measured (hexokinase method, Aeroset; Abbott Diagnostics) before ^{18}F-FDG injection. The fractional change in MR_{Glu} between ^{18}F-FDG PET at baseline and after 2 or 3 cycles of chemotherapy was calculated.

Standardized Uptake Value (SUV)

^{18}F-FDG PET scans were also evaluated semiquantitatively by SUV analysis. SUVs normalized to injected activity and patients' body weight were calculated from the mean activity concentration in the tumor VOIs between 40 and 50 min after injection, which is the last time frame of the dynamic scan. A volume-weighted mean value of each PET scan was derived from all lesions to give one average SUV (SUV_{avg}; hereafter referred to as SUV) for each PET scan. The percentage change in SUV between the ^{18}F-FDG PET at baseline and after 2 or 3 cycles of chemotherapy was calculated.

Clinical Follow-up

During and after treatment, patients were monitored with clinical examination at regular intervals, chest CT, radiography, and other imaging studies as clinically indicated. Tumor response was evaluated according to RECIST criteria without knowledge of the results of the PET studies. When recurrence was suspected or proven, patients were always restaged. The progression/relapse pattern and cause of death were determined in all cases. The date of local or distant progression was defined as the earliest date at which disease progression was confirmed, either clinically or by imaging or biopsy. Patients who were progression free at the closeout date (November 1, 2006) or who had died from any cause had their time to progression censored at that date. Survival was measured from the date of the baseline PET scan to the date of death. Patients who were still alive at the closeout date had their survival censored to that date.

Statistical Analysis

Survival and progression-free survival served as the standard of reference. Cox proportional hazards regression analysis was used to assess the predictive value of response evaluation with ^{18}F-FDG

PET, as expressed in the percentage change in MR_{Glu} and SUV between the ^{18}F-FDG PET at baseline and after 2 or 3 cycles of chemotherapy. The data have been adjusted for tumor stage at the time of the baseline PET scan. Statistical significance was assessed using the Wald χ^2 test. The overall survival and progression-free survival with respect to MR_{Glu} and SUV were calculated using Kaplan–Meier estimates. The percentage change in measurements between the first and second scan were stratified by the median value to avoid data-driven significance for the cutoff level. However, stratification at the median value is still a post hoc definition for metabolic response. To avoid this bias, also some predefined, prospective definitions of metabolic response were used. For that purpose the population was categorized according to the definitions for metabolic response of The European Organization for Research and Treatment of Cancer (EORTC), into a group with complete response (CR) or partial response (PR) ($\Delta < -25\%$), a group with stable disease (SD) ($\Delta -25\%$ to $+25\%$), and a group with progressive disease (PD) ($\Delta > +25\%$) (15). Furthermore, the population was categorized according to the cutoff values also used for size measurement (RECIST), for which $\Delta < -30\%$ is CR or PR, $\Delta -30\%$ to $+20\%$ is SD, and $\Delta > +20\%$ is PD (16). Groups were compared using the Breslow test, which counts losses that occur early in the survival distribution more heavily than losses that occur late, because sample sizes are larger in early months relative to late months. Spearman ρ-correlations were used to determine the comparability between the different methods to measure glucose metabolism. Statistical tests were based on a 2-sided significance level, and the level of significance was set at 0.05.

RESULTS

Patient Characteristics

Sixty consecutive eligible NSCLC patients were included in this prospective study. After the first ^{18}F-FDG PET, 9 patients were excluded for several reasons: technical issues ($n = 1$), refusal to undergo a second ^{18}F-FDG PET scan ($n = 2$), death before the second ^{18}F-FDG PET ($n = 1$), and early discontinuation of chemotherapy due to a significant decline in performance status ($n = 5$). Therefore, complete ^{18}F-FDG PET datasets (median interval between baseline and follow-up ^{18}F-FDG PET, 49 $\pm$ 17 d) were available in 51 patients (37 males, 14 females; mean age, 59 y; range, 38–76 y) for analysis of the predictive value. Patient characteristics are summarized in Table 1.

Treatment

Fifteen patients were treated with induction chemotherapy and 36 patients were treated in a palliative setting. Of the latter 36 patients, 32 received first-line chemotherapy and 4 received second-line chemotherapy. The chemotherapy regimens used were carboplatin/gemcitabine ($n = 27$), gemcitabine/cisplatinum ($n = 9$), carboplatin/etoposide ($n = 9$), cisplatinum/vinorelbine ($n = 2$), cisplatin/etoposide ($n = 1$), triapine/gemcitabine ($n = 1$), carboplatin/docetaxel ($n = 1$), and docetaxel ($n = 1$). After induction chemotherapy ($n = 15$), 2 patients underwent surgery, 10 patients were treated with radical radiotherapy, and 3 patients were treated with radiotherapy with palliative intent because of progression during induction chemotherapy based on CT criteria.

TABLE 1
Patient Characteristics

Characteristic	Value
Mean age	59 y (range, 38–76 y)
Men	37
Women	14
Histology	
Squamous cell carcinoma	21
Adenocarcinoma	24
Large cell carcinoma	4
Bronchoalveolar cell carcinoma	1
Clear cell carcinoma	1
Tumor differentiation	
Very poor	13
Poor	6
Intermediate	7
Well	1
Unspecified	24
Tumor stage	
IB	1
IIA	1
IIIA	8
IIIB	10
IV	31

Patient Follow-up

No patients were lost to follow-up. Median follow-up time was overall 13 mo (range, 2–48 mo), for surviving patients 20 mo (range, 9–45 mo), and for deceased patients 9 mo (2–48 mo). During this time period, 38 patients had died and tumor progression was diagnosed in 45 of the 51 patients. Median time to progression was 7 mo (range, 0–39 mo). Overall survival after baseline ^{18}F-FDG PET at 1 y was 57%, at 2 y 36%, and at 3 y 22%. Progression-free survival after baseline ^{18}F-FDG PET at 1 y was 26%, at 2 y 17%, and at 3 y 8%.

Quantitative Changes in ^{18}F-FDG Uptake

Mean MR_{glu} at baseline was 0.146 $\pm$ 0.079 $\mu mol \cdot mL^{-1} \cdot min^{-1}$ (range, 0.028–0.356) and during evaluation was 0.084 $\pm$ 0.072 $\mu mol \cdot mL^{-1} \cdot min^{-1}$ (range, 0.009–0.355). The median fractional change of MR_{glu} as compared with baseline was $-47\% \pm 55\%$ (range, -93% to $+226\%$). Mean SUV at baseline was 5.27 $\pm$ 2.51 (range, 1.37–16.66) and during evaluation was 3.72 $\pm$ 2.75 (range, 0.71–16.64). The median fractional change of SUV as compared with baseline was $-35\% \pm 42\%$ (range, -73% to $+125\%$).

Figure 1 shows a typical example of a patient with stage IV NSCLC and tumor lesions who responded to chemotherapy. There is an 82% decrease in MR_{glu} and a 65% decrease in SUV relative to baseline.

^{18}F-FDG uptake measured with simplified methods (SUV) showed a significant correlation with MR_{glu} as measured with the Patlak analysis ($r = 0.84$, $P < 0.0001$) at baseline, after 2 or 3 cycles of chemotherapy ($r = 0.93$, $P < 0.0001$), as well as in terms of fractional changes after 2 or 3 cycles of chemotherapy ($r = 0.94$, $P < 0.0001$).
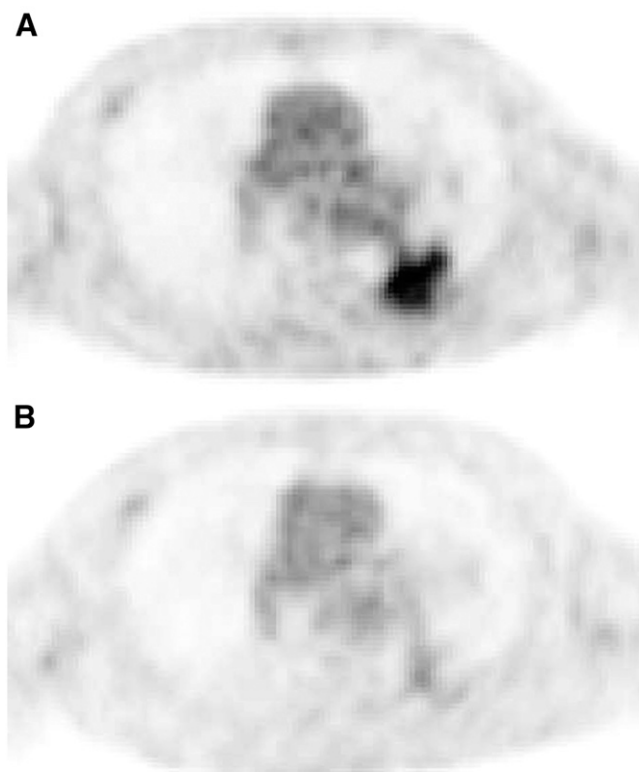
FIGURE 1. Typical example of patient with stage IV NSCLC and tumor lesions who responded to chemotherapy. Relative to baseline (A), there is an 82% decrease in MR_{glu} and a 65% decrease in SUV on ^{18}F-FDG PET after 2 cycles of carboplatin/gemcitabine (B).

Prediction of Survival by ^{18}F-FDG PET

To generate Kaplan–Meier survival curves, the decrease in tumor glucose metabolism was dichotomized at the median value, which was −47% and −35% for ΔMR_{Glu} and ΔSUV, respectively. The Kaplan–Meier survival curves for overall survival are shown in Figure 2A (ΔMR_{Glu}) and Figure 2B (ΔSUV). The difference in survival between both strata was highly significant for both ΔMR_{Glu} and ΔSUV ($P = 0.017$ for ΔMR_{Glu} and $P = 0.018$ for ΔSUV; Table 2 and Figs. 2A and

2B). For patients with a decrease in MR_{Glu} lower than the median value, median overall survival was only 8 mo, whereas it was 17 mo for patients with a more pronounced decrease in MR_{Glu}.

There was also a significant difference in progression-free survival between both groups when dichotomized at the median value of ΔMR_{Glu} ($P = 0.002$) and of ΔSUV ($P = 0.0009$) (Table 2). Patients with a decrease of MR_{Glu} by >47% were characterized by a significantly longer time to progression (median, 10 vs. 3 mo; $P = 0.002$). The results obtained for ΔSUV were also evident: median progression-free survival, 11 versus 3 mo. The corresponding Kaplan–Meier curves for progression-free survival are shown in Figure 3A (ΔMR_{Glu}) and Figure 3B (ΔSUV). There was a highly significant increase in the rates of progression associated with worsening response as assessed by PET on Cox proportional regression analysis adjusting for disease stage at the time of commencement of treatment ($P = 0.018$ for ΔMR_{Glu} and $P = 0.028$ for ΔSUV).

Applying predefined, prospective definitions of metabolic response with cutoff levels according to Young et al. (15) (EORTC) and according to the cutoff levels also used for size measurement (RECIST), the complete dataset showed similar highly significant differences in progression-free survival (Table 3). However, for prediction of overall survival, categorization according to these predefined cutoff levels showed only statistically significant differences for RECIST cutoff levels applied to ΔSUV ($P = 0.027$).

DISCUSSION

The results of this prospective study show that fractional changes in tumor glucose metabolism from baseline ^{18}F-FDG PET to ^{18}F-FDG PET after 2 or 3 cycles of chemotherapy were highly predictive for outcome in patients with NSCLC. When applying the generally used post hoc definition for metabolic response, by stratifying at the median value of ΔMR_{Glu} and ΔSUV, the difference in overall survival between both strata was highly significant ($P = 0.017$ for ΔMR_{Glu} and $P = 0.018$ for ΔSUV). Also, a
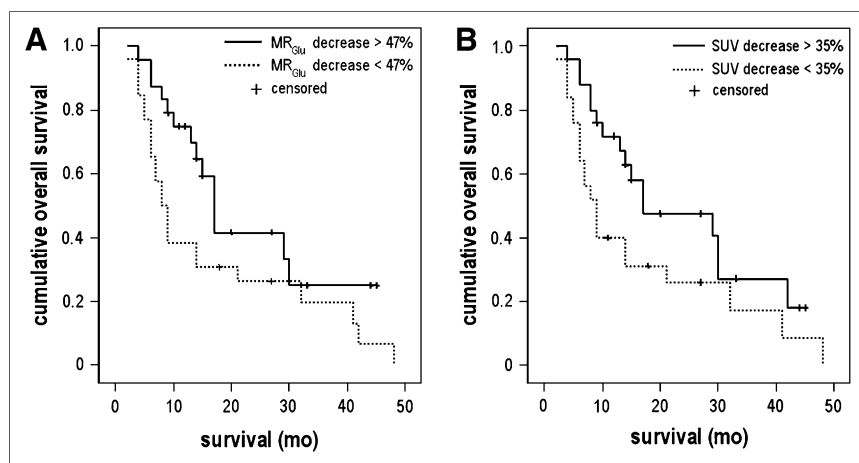

FIGURE 2. Kaplan–Meier estimates for overall survival: Kaplan–Meier analysis of relationship between overall survival and ΔMR_{Glu} (dichotomized using median value of −47%) (A) and ΔSUV (dichotomized using median value of −35%) (B).

TABLE 2
Survival Estimates

Median and 1-, 2-, and 3-y overall survival rates (OS) for strata dichotomized using median values of ΔMR_{Glu} and ΔSUV between PET scan at baseline and evaluation

Overall survival	Median OS (mo)	1-y OS (%)	2-y OS (%)	3-y OS (%)	P value
All patients	13	57	36	22	
PET response					
$\Delta MR_{Glu} < -47\%$	17	75	42	25	0.017
$\Delta MR_{Glu} > -47\%$	8	38	26	20	
$\Delta SUV < -35\%$	17	72	47	27	0.018
$\Delta SUV > -35\%$	9	40	26	17	

Median and 1-, 2-, and 3-y progression-free survival rates (PFS) for strata dichotomized using median values of ΔMR_{Glu} and ΔSUV between PET scan at baseline and evaluation

Progression-free survival	Median PFS (mo)	1-y PFS (%)	2-y PFS (%)	3-y PFS (%)	P value
All patients	7	26	17	8	
PET response					
$\Delta MR_{Glu} < -47\%$	10	34	23	8	0.002
$\Delta MR_{Glu} > -47\%$	3	15	8	4	
$\Delta SUV < -35\%$	11	41	31	19	0.0009
$\Delta SUV > -35\%$	3	12	4	0	

difference in progression-free survival was seen ($P = 0.002$ for ΔMR_{Glu} and $P = 0.0009$ for ΔSUV).

The strength of the present study is that also some pre-defined, prospective definitions of metabolic response were evaluated, comparing 3 strata for assessment of metabolic changes by ^{18}F-FDG PET. One of these prospective definitions was proposed by the EORTC (15) to provide a framework for comparison between studies and to facilitate assessment of the technique. A >25% decrease in glucose metabolism was estimated to be a sign of partial metabolic response after 2 or more cycles of chemotherapy. According to this EORTC definition, the present study demonstrated highly significant differences in progression-free survival between each stratum ($P = 0.007$ for ΔMR_{Glu} and $P = 0.0003$ for ΔSUV). The same significant results were found when using the cutoff levels that are proposed for evaluation after 1 cycle of chemotherapy, for which a metabolic response is defined by a decrease in tumor glucose metabolism of >15%. However,

for prediction of overall survival using these EORTC criteria, no statistical significance was reached; only a trend was found ($P = 0.0504$). This is probably due to the limited number of patients in each stratum: more censored patients for overall survival compared with progression-free survival in combination with smaller groups due to categorization into 3 groups (CR or PR, SD, and PD) instead of 2. The EORTC PET response criteria were developed by consensus between a range of PET experts and currently represent the most authoritative SUV-based recommendations. Also, when applying the same cutoff levels that are used for size measurement in standard clinical response assessment with conventional methods according to RECIST (16,17), significant differences between the strata were found in progression-free survival as well as overall survival with respect to ΔSUV.

These results imply that measurement of treatment-induced changes in tumor glucose metabolism with PET is quite robust. There is even more considerable evidence

FIGURE 3. Kaplan–Meier estimates for progression-free survival: Kaplan–Meier analysis of relationship between progression-free survival and ΔMR_{Glu} (dichotomized using median value of −47%) (A) and ΔSUV (dichotomized using median value of −35%) (B).
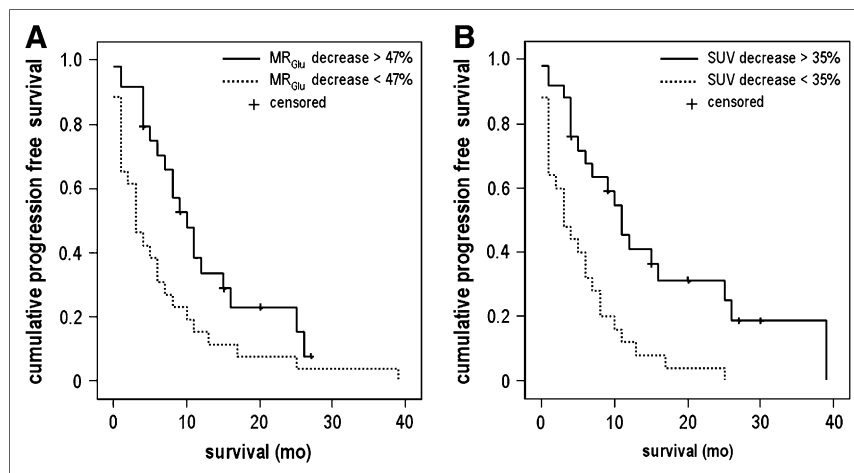
TABLE 3
Progression-Free Survival Estimates for Predefined Metabolic Response Categories

Median and 1-, 2-, and 3-y progression-free survival rates (PFS) for EORTC metabolic response categories					
	Median PFS (mo)	1-y PFS (%)	2-y PFS (%)	3-y PFS (%)	P value
CR/PR: $\Delta MR_{Glu} < -25\%$	8	33	19	9	0.007
SD: ΔMR_{Glu} −25% to +25%	3	9	0	0	
PD: $\Delta MR_{Glu} > +25\%$	1	0	0	0	
CR/PR: $\Delta SUV < -25\%$	11	39	26	16	0.0003
SD: ΔSUV −25% to +25%	3	13	6	0	
PD: $\Delta SUV > +25\%$	0	0	0	0	

Median and 1-, 2-, and 3-y progression-free survival rates (PFS) for metabolic response categories applying cutoff levels that are used for clinical response with conventional methods (size measurement) according to RECIST					
	Median PFS (mo)	1-y PFS (%)	2-y PFS (%)	3-y PFS (%)	P value
CR/PR: $\Delta MR_{Glu} < -30\%$	10	36	21	10	0.006
SD: ΔMR_{Glu} −30% to +20%	3	9	0	0	
PD: $\Delta MR_{Glu} > +20\%$	1	0	0	0	
CR/PR: $\Delta SUV < -30\%$	11	42	28	17	0.0003
SD: ΔSUV −30% to +20%	3	11	0	0	
PD: $\Delta SUV > +20\%$	0	0	0	0	

for this, as simplified ^{18}F-FDG PET measures (SUV) and the more complex, quantitative measures, derived from Patlak graphical analysis (MR_{Glu}), show comparable highly significant results indicative for treatment outcome. Given the high correlation between ΔSUV and ΔMR_{Glu} ($r = 0.94$, $P < 0.0001$), there is no obvious need to apply the more complex dynamic imaging protocols (necessary for MR_{Glu} calculation) for prediction of therapy response in monitoring chemotherapy of NSCLC. This indicates that ^{18}F-FDG PET can be readily implemented as a routine clinical tool for response monitoring when some basic requirements of quality assurance are met (18). Multiple follow-up scans encourage a simplified approach to improve patient compliance, an important feature of successful clinical trials. Another advantage of the SUV is that it can be calculated from static whole-body ^{18}F-FDG PET studies. In quantitative dynamic scans, only one axial field of view of typically 15–20 cm can be studied during the dynamic data acquisition. As metastatic lesions in different parts of the body may respond differently to chemotherapy, this represents a principal advantage of SUV.

The results of the present study are in line with other studies on the predictive value of ^{18}F-FDG PET in locally advanced NSCLC. Several studies indicated a possible role for PET in assessment of response during or after radiotherapy (19), induction chemotherapy (20–22), or a combination thereof (8,23–27). The earliest study, performed in 1996 by Ichiya et al. (19), showed a more prominent decrease in ^{18}F-FDG uptake in patients with a radiotherapy response on CT compared with those with no change in tumor size on CT. In the pilot study of Vansteenkiste et al. (20), a reduction in ^{18}F-FDG uptake of >50% in the primary tumor or mediastinal clearance after induction chemotherapy proved to be a better predictor of long-term

survival compared with the World Health Organization criteria (28,29) used as the standard for response assessment on CT. Another study that evaluated response monitoring of induction chemotherapy (21) showed that ^{18}F-FDG PET identified prognostically different strata in patients considered responsive according to CT. In this prospective multicenter study, ^{18}F-FDG PET was performed before and after 1 and 3 cycles of induction chemotherapy. The residual metabolic rate of glucose after 1 cycle selected patients with different outcomes. The residual metabolic rate of glucose after completion of induction chemotherapy proved to be the best prognostic factor. The other 6 studies (8,23–27) showed that ^{18}F-FDG PET was also predictive with respect to therapy outcome of combined modality therapy. Metabolic response proved to be associated with pathologic response (23,24,26,27). A study performed by Mac Manus et al. (25) showed a significantly longer median survival for patients with complete metabolic response than for patients with incomplete metabolic response (31 vs. 11 mo).

The experience with ^{18}F-FDG PET on therapy response monitoring in advanced stages of NSCLC is limited. So far, a single well-designed study on response assessment in advanced stages (stage IIIB or IV), using serial PET scans, was performed by Weber et al. (30). Fifty-seven patients scheduled to undergo platinum-based chemotherapy were studied before and after the first cycle of therapy. A decrease in SUV of 20% or more after 1 cycle of chemotherapy was associated with a longer time to progression (163 vs. 54 d) and longer median overall survival time (252 vs.151 d). The 1-y survival rate was also significantly higher in metabolic responders compared with nonresponders (44% vs. 10%). This study showed that a reduction of metabolic activity already after 1 cycle of chemotherapy is closely correlated with final outcome of therapy.

CONCLUSION

These findings in advanced stages of NSCLC in combination with the results of the studies in locally advanced NSCLC indicate that PET may be used to predict the clinical outcome of chemotherapy. The SUV proved to be a robust parameter to detect a metabolic response. As no sophisticated methods for data analysis are required, the use of ^{18}F-FDG PET for therapy monitoring seems clinically feasible.

REFERENCES

1. Verhagen AF, Bootsma GP, Tjan-Heijnen VC, et al. FDG-PET in staging lung cancer: how does it change the algorithm? *Lung Cancer.* 2004;44:175–181.
2. van Tinteren H, Hoekstra OS, Smit EF, et al. Effectiveness of positron emission tomography in the preoperative assessment of patients with suspected non-small-cell lung cancer: the PLUS multicentre randomised trial. *Lancet.* 2002;359:1388–1393.
3. Pieterman RM, van Putten JW, Meuzelaar JJ, et al. Preoperative staging of non-small-cell lung cancer with positron-emission tomography. *N Engl J Med.* 2000;343:254–261.
4. Ashamalla H, Rafla S, Parikh K, et al. The contribution of integrated PET/CT to the evolving definition of treatment volumes in radiation treatment planning in lung cancer. *Int J Radiat Oncol Biol Phys.* 2005;63:1016–1023.
5. Juweid ME, Cheson BD. Positron-emission tomography and assessment of cancer therapy. *N Engl J Med.* 2006;354:496–507.
6. De Ruysscher D, Wanders S, van Haren E, et al. Selective mediastinal node irradiation based on FDG-PET scan data in patients with non-small-cell lung cancer: a prospective clinical study. *Int J Radiat Oncol Biol Phys.* 2005;62:988–994.
7. van Der Wel A, Nijsten S, Hochstenbag M, et al. Increased therapeutic ratio by 18FDG-PET CT planning in patients with clinical CT stage N2-N3M0 non-small-cell lung cancer: a modeling study. *Int J Radiat Oncol Biol Phys.* 2005;61:649–655.
8. Mac Manus MP, Hicks RJ, Matthews JP, et al. Positron emission tomography is superior to computed tomography scanning for response-assessment after radical radiotherapy or chemoradiotherapy in patients with non-small-cell lung cancer. *J Clin Oncol.* 2003;21:1285–1292.
9. Vansteenkiste J, Fischer BM, Dooms C, Mortensen J. Positron-emission tomography in prognostic and therapeutic assessment of lung cancer: systematic review. *Lancet Oncol.* 2004;5:531–540.
10. Sekine I, Tamura T, Kunitoh H, et al. Progressive disease rate as a surrogate end-point of phase II trials for non-small-cell lung cancer. *Ann Oncol.* 1999;10:731–733.
11. Clinical practice guidelines for the treatment of unresectable non-small-cell lung cancer: Adopted on May 16, 1997 by the American Society of Clinical Oncology. *J Clin Oncol.* 1997;15:2996–3018.
12. de Geus-Oei LF, Visser EP, Krabbe PF, et al. Comparison of image-derived and arterial input functions for estimating the rate of glucose metabolism in therapy-monitoring ^{18}F-FDG PET studies. *J Nucl Med.* 2006;47:945–949.
13. Patlak CS, Blasberg RG, Fenstermacher JD. Graphical evaluation of blood-to-brain transfer constants from multiple-time uptake data. *J Cereb Blood Flow Metab.* 1983;3:1–7.
14. Hoekstra CJ, Hoekstra OS, Stroobants SG, et al. Methods to monitor response to chemotherapy in non-small cell lung cancer with ^{18}F-FDG PET. *J Nucl Med.* 2002;43:1304–1309.
15. Young H, Baum R, Cremerius U, et al. Measurement of clinical and subclinical tumour response using [^{18}F]-fluorodeoxyglucose and positron emission tomography: review and 1999 EORTC recommendations—European Organization for Research and Treatment of Cancer (EORTC) PET Study Group. *Eur J Cancer.* 1999;35:1773–1782.
16. Therasse P, Arbuck SG, Eisenhauer EA, et al. New guidelines to evaluate the response to treatment in solid tumors: European Organization for Research and Treatment of Cancer, National Cancer Institute of the United States, National Cancer Institute of Canada. *J Natl Cancer Inst.* 2000;92:205–216.
17. Therasse P, Eisenhauer EA, Verweij J. RECIST revisited: a review of validation studies on tumour assessment. *Eur J Cancer.* 2006;42:1031–1039.
18. Westerterp M, Pruim J, Oyen W et al. Quantification of FDG PET studies using standardised uptake values in multi-centre trials: effects of image reconstruction, resolution and ROI definition parameters. *Eur J Nucl Med Mol Imaging.* 2007;34:392–404.
19. Ichiya Y, Kuwabara Y, Sasaki M, et al. A clinical evaluation of FDG-PET to assess the response in radiation therapy for bronchogenic carcinoma. *Ann Nucl Med.* 1996;10:193–200.
20. Vansteenkiste JF, Stroobants SG, De Leyn PR, Dupont PJ, Verbeken EK. Potential use of FDG-PET scan after induction chemotherapy in surgically staged IIIa-N2 non-small-cell lung cancer: a prospective pilot study—The Leuven Lung Cancer Group. *Ann Oncol.* 1998;9:1193–1198.
21. Hoekstra CJ, Stroobants SG, Smit EF, et al. Prognostic relevance of response evaluation using [^{18}F]-2-fluoro-2-deoxy-D-glucose positron emission tomography in patients with locally advanced non-small-cell lung cancer. *J Clin Oncol.* 2005;23:8362–8370.
22. Eschmann SM, Friedel G, Paulsen F, et al. Repeat ^{18}F-FDG PET for monitoring neoadjuvant chemotherapy in patients with stage III non-small cell lung cancer. *Lung Cancer.* 2007;55:165–171.
23. Choi NC, Fischman AJ, Niemierko A, et al. Dose-response relationship between probability of pathologic tumor control and glucose metabolic rate measured with FDG PET after preoperative chemoradiotherapy in locally advanced non-small-cell lung cancer. *Int J Radiat Oncol Biol Phys.* 2002;54:1024–1035.
24. Cerfolio RJ, Bryant AS, Winokur TS, Ohja B, Bartolucci AA. Repeat FDG-PET after neoadjuvant therapy is a predictor of pathologic response in patients with non-small cell lung cancer. *Ann Thorac Surg.* 2004;78:1903–1909.
25. Mac Manus MP, Hicks RJ, Matthews JP, Wirth A, Rischin D, Ball DL. Metabolic (FDG-PET) response after radical radiotherapy/chemoradiotherapy for non-small cell lung cancer correlates with patterns of failure. *Lung Cancer.* 2005;49:95–108.
26. Pottgen C, Levegrun S, Theegarten D, et al. Value of ^{18}F-fluoro-2-deoxy-D-glucose-positron emission tomography/computed tomography in non-small-cell lung cancer for prediction of pathologic response and times to relapse after neoadjuvant chemoradiotherapy. *Clin Cancer Res.* 2006;12:97–106.
27. Yamamoto Y, Nishiyama Y, Monden T, et al. Correlation of FDG-PET findings with histopathology in the assessment of response to induction chemoradiotherapy in non-small cell lung cancer. *Eur J Nucl Med Mol Imaging.* 2006;33:140–147.
28. Miller AB, Hoogstraten B, Staquet M, Winkler A. Reporting results of cancer treatment. *Cancer.* 1981;47:207–214.
29. Green S, Weiss GR. Southwest Oncology Group standard response criteria, endpoint definitions and toxicity criteria. *Invest New Drugs.* 1992;10:239–253.
30. Weber WA, Petersen V, Schmidt B, et al. Positron emission tomography in non-small-cell lung cancer: prediction of response to chemotherapy by quantitative assessment of glucose use. *J Clin Oncol.* 2003;21:2651–2657.